PERGAMON

International Journal of Multiphase Flow 25 (1999) 1545–1559

International Journal of Multiphase Flow

www.elsevier.com/locate/ijmulflow

Experimental investigation of the impaction of water droplets on cylindrical objects

L.S. Hung*, S.C. Yao

Department of Mechanical Engineering, Carnegie Mellon University, Pittsburgh, PA 15213-3890, USA

Received 26 January 1998; received in revised form 13 December 1998

Abstract

The impaction of water droplets on isothermal cylindrical wires has been investigated experimentally in the present study. Mono-size droplets of 110, 350 and 680 μm in diameter were generated using piezoelectric droplet generators. The effects of droplet velocity and wire size were varied parametrically to reveal the impacting phenomena. Typical modes of the impaction outcome are disintegration and dripping. For droplets impacting on small wires, finer drops are disintegrated if the impacting droplet velocity is high, and larger dripping drops are observed if the velocity is low. For droplets impacting on large wires, bigger pendent drops are gradually formed which would eventually detach from the wires under the influence of gravity. In addition, droplets impacting on wires with waxy surface generate smaller dripping drops than that of the non-waxed wires. A non-dimensional regime map and new formulations in terms of the droplet Weber number, the wire Bond number and the size ratio of the wire diameter to incoming droplet diameter have been established to identify the regime for each mode of outcome and to predict the size of the dripping drops within the experimental limits.

Keywords: Mono-size droplets; Impaction; Cylindrical objects; Dripping

1. Introduction

The impaction of droplets on objects are widely encountered in a variety of industrial processes. Typical applications are found in the quenching of hot metal strips by spray cooling,

* Corresponding author. Present address: Delphi Automotive Systems, P.O. Box 20366, Rochester NY 14602-0366, USA.

0301-9322/99/$ - see front matter
PII: S0301-9322(98)00085-8

the thin coatings on surfaces at spray painting, and the molten droplets impinging on substrate during spray forming. The outcome of the impaction is very much dependent upon the condition of the incoming droplets and the configuration of the impacted surfaces. Since the impaction process involves complex mechanisms, research effort has been placed on revealing the fundamental behavior of droplets impacting on infinitely large solid surfaces.

Extensive studies have been made on the impacting phenomena of droplets onto large planar solid surfaces (Harlow and Shannon, 1967; Lesser, 1981; Cazabat, 1987; Yao and Cai, 1988; Chandra and Avedisian, 1991; Cohen, 1991; Karl et al., 1994; Fukai et al., 1995; and Zhao et al., 1996a,b). Various approaches, such as sequential photographic technique, high speed photography, digital imaging analysis, numerical computation and analytical modeling have been undertaken to study the spreading behavior, the contact angle, the angle of impact, the wetting effect, the breakup and disintegration, the deformation profile, and the fluid dynamics of the impacting droplets. A comprehensive review by Rein (1993) presented the phenomena of liquid drops impacting on both solid and liquid surfaces. He concluded that the outcome of droplet impaction depends on the properties of the droplet, the droplet impact velocity, the condition of the impacted surface, and the ambient fluid. Particularly at the early stage of droplets impacting on flat surface, the deformation process depends on the fluid properties such as the density, surface tension and viscosity, and the contact angle at the liquid–solid interface. Viscous forces within the drop act to absorb the kinetic energy during the spreading and bouncing processes. The impacting phenomena could include a combination of bouncing, spreading, splashing and coalescence.

In many other situations, the geometry of the impacted surface may be very complex and far from being planar. For example, in agricultural applications, pesticide sprays are targeted to cover the plants such as crops, leaves and stems, all with very complex geometric shapes and sizes. The impaction of fine pesticide droplets on the leaf surface has been studied extensively to enhance the retention of droplets from bouncing off the surface. During impact, the inertia of the droplet will make it spread out laterally over the surface and the dynamics of the deformation of the droplets depends on its kinetic energy and surface tension (Spillman, 1984). The microstructure of the surface greatly affects whether the impinging drops reflect or are retained by the surface (Reichard et al., 1986; Crease et al., 1991). Droplets are more likely to bounce from a smooth waxy surface than from rough surface. Therefore, in order to enhance the magnitude of deposition, electrostatic charging of individual droplets has also been applied to enhance the retention of droplet on the plants (Hislop, 1988). When the droplets collide with these surfaces, the spreading and the splashing characteristics would be quite different and the results of droplets impacting on planar surfaces may not be applicable to the non-planar cases.

In contrast, very limited published literature is available on droplets impacting on non-planar surfaces. An early study by Levin and Hobbs (1971) used a high speed camera to examine the droplets impacting on a curved wall with the radius of curvature much larger than that of the droplet. Later, Dear and Field (1988) also investigated the surface geometry effect in liquid/solid impact using high speed photography to study the propagation of shock waves in both the liquid and the impacted medium. More recently, Bussmann et al. (1997) studied the phenomena of a single 2 mm water droplet impacting on an arbitrary surface geometry such as a 45° inclined flat surface or a sharp edge. They suggested that the phenomena of droplets

impacting on these arbitrary surfaces were very different than those of the typical flat surface impacting situation.

In the above published studies, the droplets are usually very small compared to the dimension of the impacted surface. Very little information has been reported on droplets hitting on surfaces with finite dimensions which are comparable to the sizes of the droplets. A relevant work in this area was performed by Yao et al. (1988). They studied the phenomena of droplets impacting on thin rectangular strips which were heated beyond the Leidenfrost temperature. They showed that when the droplet diameter and the strip thickness were comparable, the impacting phenomena included a combination of splashing and cutting. Recently, Liu et al. (1994) performed a numerical study to examine the spreading behavior and consolidation of molten droplets impinging on a waved target surface. They concluded that when the droplet impacted on a waved surface, it spread out laterally and maintained a relatively good adhesive contact with the waved surface. Through these preliminary studies, it is expected that the geometry and size of the impacted surface would play a significant part in the outcome of the droplet impacting phenomena.

In addition, the velocity of the drop plays a critical role because it affects the magnitude of impact onto the wire. Later on when the drop is about to detach from the wire, surface tension becomes important to hold the dripping drop in a spherical shape. Therefore, the effects of inertia and surface tension are considered in the overall dripping process. Even though the effects of viscosity in terms of Reynolds number and measure of interfacial contact angle are not considered in the current investigation, they will be left for future effort.

The present work explores the impaction of water droplets on non-planar objects with finite dimensions, which has not been reported in much detail. Therefore, the objective of this study is to experimentally investigate the phenomena of droplets impacting on cylindrical wires (Fig. 1). Distilled water is chosen for this investigation such that the effect of inertia in terms of Weber number can be established systematically by varying the velocity of the impacting drop within our experimental limits. An impulsed liquid spray generator is used to generate the

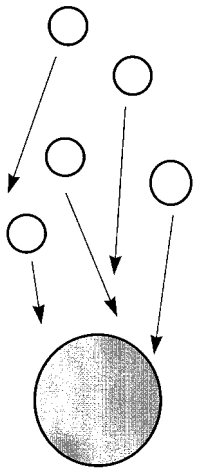

Fig. 1. Schematic diagram of droplets impacting on a horizontal wire.

mono-size droplets. A photographic technique with digital image processing is employed to examine the phenomena of droplets impacting on wires which are located horizontally. The effects of the droplet impacting velocity and the wire size on the droplet impaction are revealed parametrically. In addition, the dripping drop size measurement on waxed wires will also be examined briefly. The resulting droplet behavior is explored with the non-dimensional representations of the collected data. New regime map and correlations based on the non-dimensional parameters are also established to provide quantitative analysis for the outcome of the impacting process.

2. Experimentation

2.1. Experimental apparatus

Fig. 2 shows the schematic diagram of the overall experimental setup. Its main components are the mono-size droplet stream generator, the distilled water loop, and the image recording unit for data display and analysis.

The mono-size water droplet stream was generated using the modified design of the impulsed liquid spray generator developed by Ashgrizzadeh and Yao (1983). This droplet generator

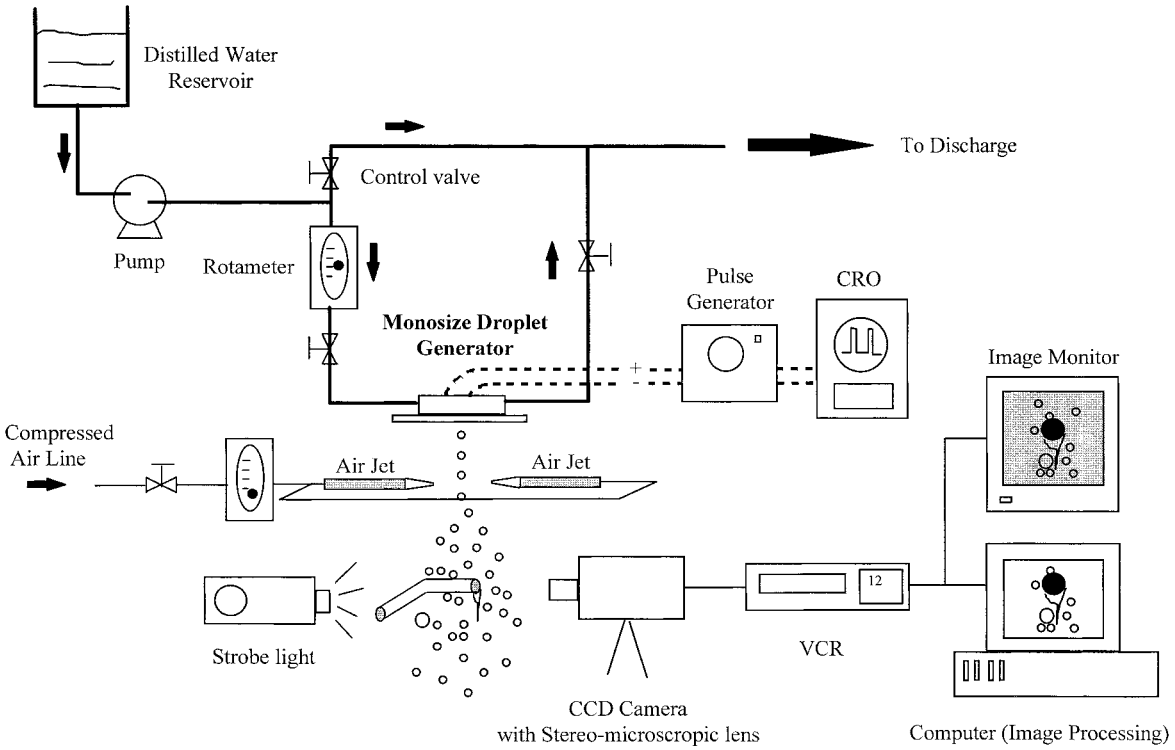

Fig. 2. Schematic diagram of the overall setup.

consisted of a fluid chamber, a thin piezoelectric plate mounted on top, and a nozzle plate mounted at the bottom. During the experiment, distilled water from the liquid reservoir was pumped into the droplet generator. A rotameter with a control valve was used to regulate the volumetric flow rate. As the fluid chamber was pressurized, a water jet was formed through the glass nozzle. Electric pulses from the pulse generator were applied to the piezoelectric plate. The pulses caused the piezoelectric plate to vibrate and hence created a disturbance that was imposed onto the water jet. The jet then broke up into a fine droplet stream with uniform size, spacing and velocity.

The droplet stream was then perturbed by two small opposing air jets so that the droplets became more randomly spread over the region where they approached the wire. The wire was located at about 10 cm below the nozzle and was bent into an L-shape. The viewing direction of the camera was taken from the end along the wire. The images of the impacting phenomena were displayed on a high resolution image monitor using a CCD camera equipped with a high magnification stereo-microscopic lens and were recorded simultaneously on a video tape by a VCR. The illumination was provided by a background strobe light. The selected images from the video tape were captured into a Pentium Pro 200 MHz computer through a frame grabber. These images were then analyzed frame by frame through digital image processing.

Digital images were used mainly for measuring the size of the droplets hanging and dripping from the wire. After a known length had been defined for calibration, this calibrated scale was then applied to measure the diameter of the dripping drops. A minimum of five pictures of each condition were used to obtain a representative averaged data measurement.

In addition, the droplet generator was also modified to operate at a drop-on-demand mode. Instead of producing a continuous stream of mono-size droplets, it was capable of generating individual droplets with a superb control over the droplet injecting frequency. Its components were almost identical to the droplet stream generator described in previous section. As a single electric pulse was applied to the piezoelectric crystal plate, the plate vibrated once accordingly. The vibration produced a repulsive force at the nozzle exit through the fluid chamber to form a single droplet. This droplet generator was able to produce droplets at a rate up to 10 Hz.

Unlike the droplet stream generator, this drop-on-demand generator required an extremely careful control on the pressure balance between the reservoir and the nozzle exit. In addition, the voltage supplied to the piezoelectric vibration was quite high, typically ranging from 50 to 80 VDC peak-to-peak. Details of the design for both droplet generators can be found in work by Hung (1998).

2.2. Experimental conditions

Mono-size water droplets of 350 μm in diameter were generated using the droplet stream generator. The velocity of the droplet was determined by measuring the jet diameter and the volume flux which gave the incoming velocity ranging between 2.8 and 7.0 m/s. The corresponding excitation frequency of the piezoelectric transducer was varied from 3600 to 10,000 Hz. Four velocities of the droplets were produced for the impaction studies which corresponded to the droplet Weber number conditions of 41, 98, 172 and 230. Seven standard stainless steel wires of various diameters were selected in the present investigation: 113, 254, 381, 508, 813, 1190 and 1588 μm. The volumetric flux was measured to be 17.6 $cm^3/min/cm^2$

and was maintained for all the experiments. In another study, a single stream droplet with larger diameter of about 680 μm was also generated. The incoming velocity of the droplet stream was about 2.0 m/s, and the corresponding droplet Weber number was 37.9. In the case of single droplet impaction, droplets with diameter of 110 μm and velocity about 1 m/s were produced that corresponded to the droplet Weber number of about 4.

3. Results and analysis

3.1. Non-dimensional parameters

The controlling parameters of the impacting phenomena in this study are the incoming droplet diameter (d), fluid properties of the droplet (μ, σ, ρ_L), incoming droplet velocity (V_0), and the wire diameter (D). In addition, the dripping drop may be formed gradually beneath the wire under the influence of gravity in some cases. Therefore, the gravitational constant (g) and the size of the dripping drop (D') are also considered in the analysis. Fig. 3 shows the schematic drawing of the impacting situation.

A more generalized representation of these parameters can be grouped into four non-dimensional forms, namely, the droplet Weber number (We), the size ratio of wire diameter to the incoming droplet diameter (R), the size ratio of the dripping drop to the wire diameter (R'), and the wire Bond number (B) with the following definitions:

$$We = \frac{\rho_L V_0^2}{(\sigma/d)} \tag{1}$$

$$R = \frac{D}{d} \tag{2}$$

$$R' = \frac{D'}{D} \tag{3}$$

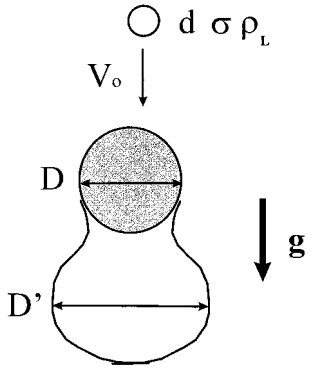

Fig. 3. Physical parameters for the impacting situation.

$$B = \frac{D}{\sqrt{(\sigma/g\rho_L)}} \tag{4}$$

The droplet Weber number can be considered as the ratio of the kinetic energy to the surface energy of the drop. The wire Bond number represents the ratio of the gravitational force to surface tension. This Bond number is a key parameter in the analysis when the effect of gravity is considered for the drops dripping under the wire.

3.2. The impaction phenomena

Generally, when the droplets impact on the wire, they have a tendency to wet and stick to the surface. The contact usually creates a thin liquid film on the wire. Depending on the size of the wire, this thin film may either break up into smaller drops if the wire is small, or it may grow into a ligament hanging beneath the wire if the wire is large. This ligament may evolve into a wriggling fragment or a pendent drop profile which eventually would detach from the wire. Fig. 4 shows the typical classifications of the droplet impacting phenomena on wires within our experimental limits, which are the disintegration mode, the momentum induced dripping mode, and the gravity induced dripping mode.

The disintegration mode occurs primarily when the droplets of moderate impacting velocity come into contact with a wire which is smaller than the incoming droplet. If the droplet velocity is very high, this mode would also happen even if the wire is larger than the droplet. As shown in Fig. 4A, when the droplets impact onto the surface of the wire, the wire serves as a shearing or cutting medium to the droplet. The minimal contact between the droplets and the wire causes a small surface tension effect at the interface. The water film being developed on the wire warps around the top portion of the wire and forms a "V" shaped fragment. It splits into two halves, one on each side. Each small fragment behaves like a small water jet and emerges directly outward. Eventually, each thin liquid jet disintegrates into even smaller drops.

Figs. 4B and C demonstrate the phenomena of drops dripping from the bottom of the wire. This observation can be divided into two modes: (1) momentum induced dripping mode, and (2) gravity induced dripping mode. These modes are usually observed when the wire is larger than the droplet size. The gravity induced dripping resembles the situation of dropwise condensation from the bottom of the horizontal tubes.

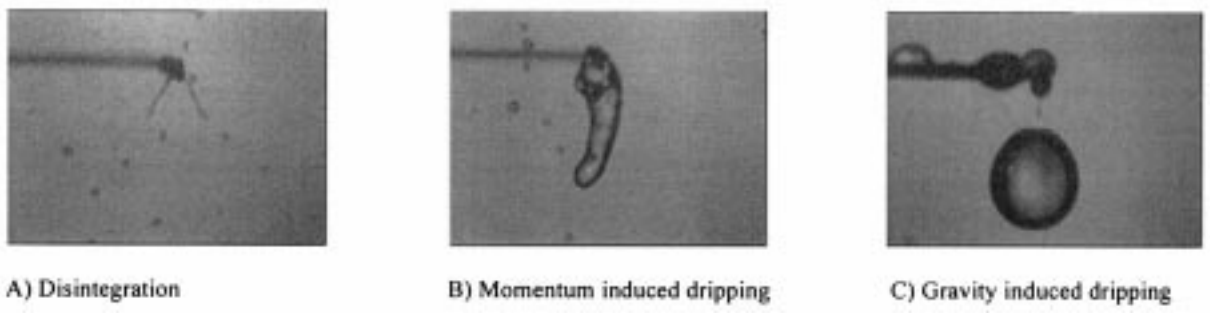

Fig. 4. Typical classifications of the droplet impacting phenomena.

In the momentum induced dripping mode, when the incoming droplets make contacts with the wire, a water film builds up consistently. The film runs off the contact point and wraps around the wire from both sides, and finally the film reattaches and forms a large fragment beneath the wire. There are two reasons for which a longer and thicker fragment is formed. Firstly, the water film carries downward momentum from the top side of the wire; and secondly, droplets may impact on this ligament directly without hitting the wire. The shape of this fragment is very irregular. As the fragment becomes larger, it wriggles more vigorously under the influence of gravity as well as the momentum added by the impacting droplets. Finally, the surface tension at the interfacial contact can no longer sustain the combined effect of the weight and the downwards force of the impacting drops on the ligament. At this point, the drop detaches and falls off the wire.

In the gravity induced dripping mode, the formation process of the dripping drops is very similar to the previous case. However, the shapes of the dripping drops are much more spherical. The liquid feeding into the ligament carries less downward momentum due to larger size of the wire or lower droplet velocities. As a result, the shape of the ligament resembles the form of a pendent drop. Eventually, when its weight is large enough to overcome the surface tension at the wire interfacial surface, the drop detaches from the wire and drips off at gravity. The size of the dripping drops in this case is usually larger than the ones in the case of momentum induced dripping. Occasionally, there are some secondary drops formed when the primary pendent drop detaches from the wire.

Fig. 5 shows the typical impacting phenomena as a function of wire size from 113 to 1588 μm and the droplet Weber number from 41 to 230. The incoming droplet size is 350 μm for all these cases. Disintegration occurs consistently when the droplets impact on the 113 μm wire ($R = 0.34$), regardless of the Weber number condition. For a larger wire diameter of 254 μm, disintegration only occurs at the higher Weber numbers of 172 and 230. For even larger wires of 381 and 508 μm, disintegration only appears at the highest Weber number of 230. At the wire size of 813 μm and larger, no more droplet disintegration is observed.

The phenomenon of momentum induced dripping also occurs in a limited range of droplet Weber number and wire size. At the lowest Weber number of 41, all dripping drops tend to be gravity-induced. At the Weber number of 97, droplets impacting on wires with diameter of 254, 381, and 508 μm give rise to momentum induced dripping drops. At a higher Weber number of 172, similar phenomena also occur at larger wire sizes of 381 and 508 μm. As the Weber number further increases to 230, only the wire of 813 μm would result in the momentum induced dripping phenomena. All other cases of droplets dripping from the wires show a reasonably spherical form of the pendent drops, indicating the situation of gravity induced dripping mode.

Fig. 6 shows the dripping drops phenomenon of single droplets impacting on wires at the drop-on-demand condition. The droplets are approximately 110 μm in diameter moving downward at about 1 m/s. They impact on the wires directly without the influence of the air jets. The droplet Weber number is about 4.0. At such a low Weber number condition, the droplet has very little inertial force and the interfacial contact is dominated by the surface tension effect. As shown in Fig. 6, the profile of the hanging drops highly resembles the pendent drop situation. This suggests that the dripping phenomenon is a pure gravity-induced situation. In general, due to a larger interfacial contact area, the dripping drops are larger as

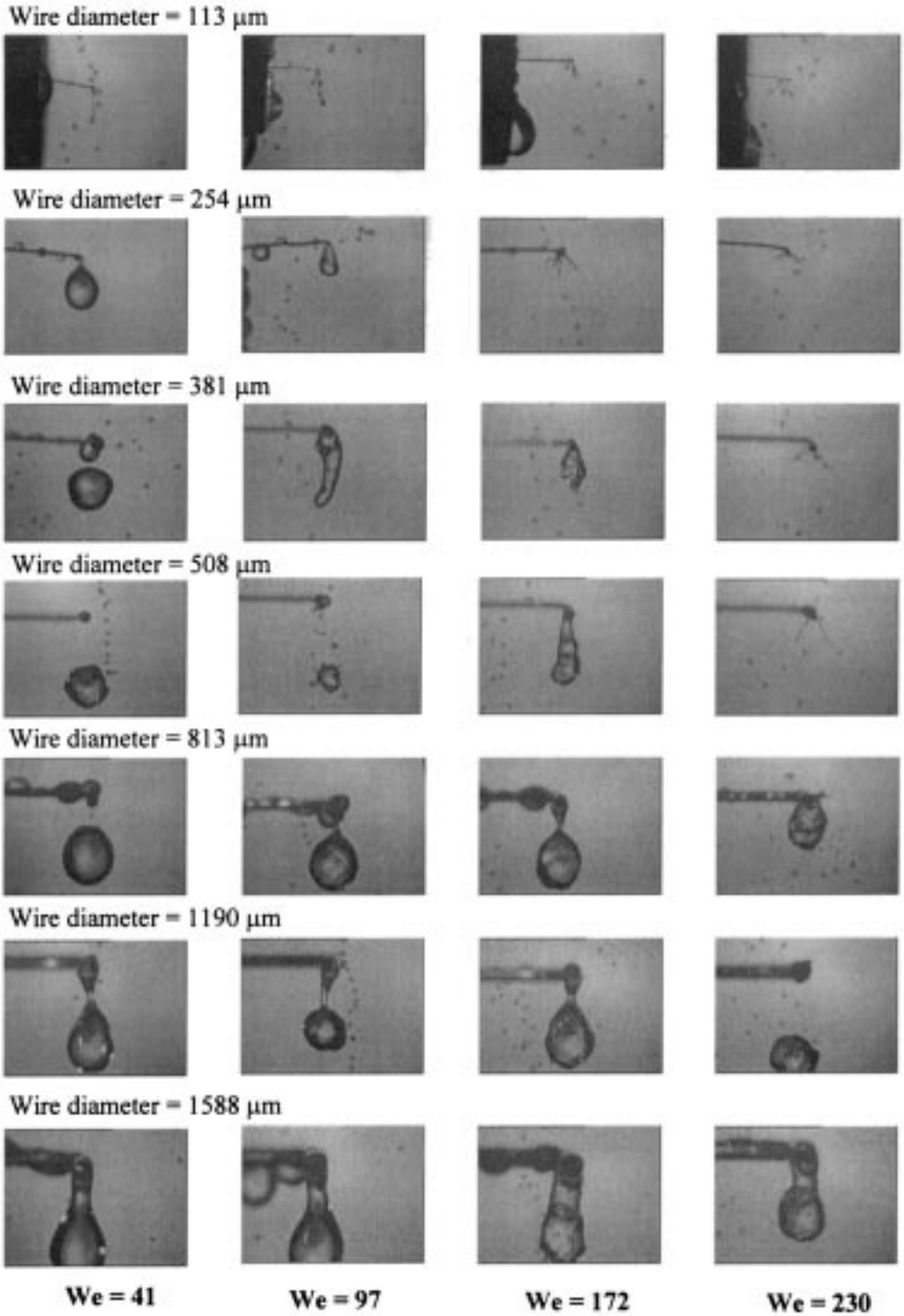

Fig. 5. Phenomena of droplets impacting on wires (incoming droplet diameter = 350 μm).

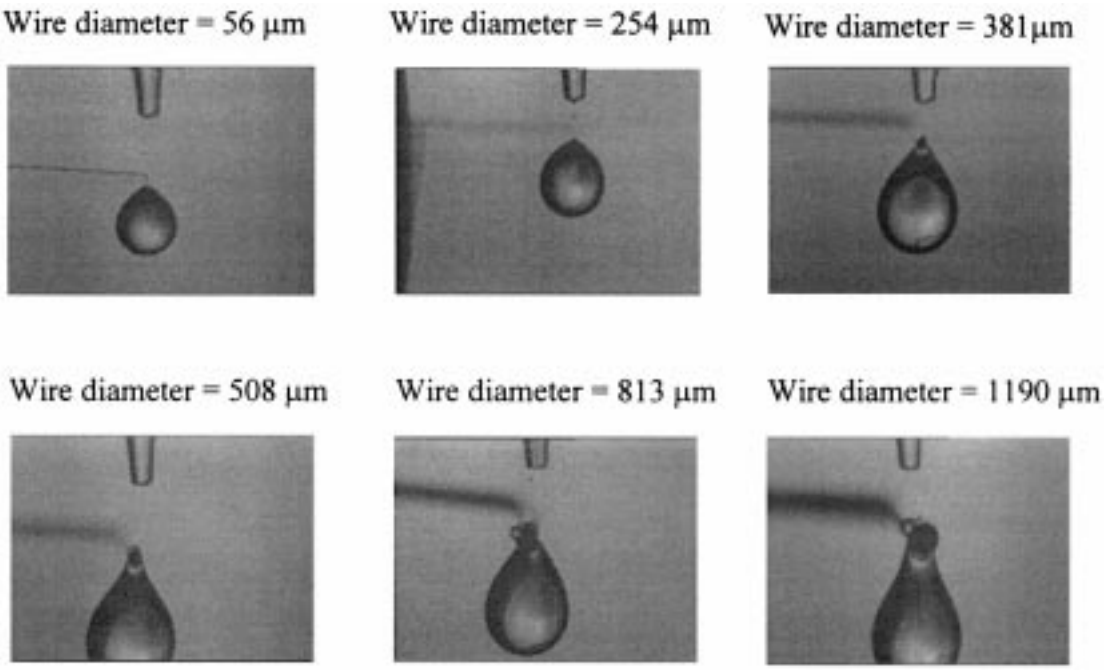

Fig. 6. Phenomenon of droplets hanging on wires (drop-on-demand mode) (droplet Weber number = 4, incoming droplet diameter = 110 μm).

the wire size increases. Once the volume of the pendent drop reaches a critical value, necking begins near the contact point and the drop detaches from the wire.

A regime map is obtained to provide an overall quantitative analysis for the outcome of the impacting process at the conditions studied. This is presented non-dimensionally in terms of the incoming droplet Weber number (We) and the size ratio of wire diameter to droplet diameter (R). This regime map is shown in Fig. 7.

On the regime map, the square symbols represent the disintegration mode (Regime I), the triangle symbols are for the momentum induced dripping mode (Regime II), and the circle symbols are for the gravity induced dripping mode (Regime III). Two lines are used to divide the different regimes. The boundaries of the zones in the map are not sharp, but they can be used as a first order criterion for predicting the impacting outcome of other similar processes.

3.3. The dripping drops

As reported earlier, dripping drops are frequently observed due to the formation of the liquid fragment under the wire. It is therefore of interest to quantify the size of the dripping drops as a function of the wire size and Weber number.

From the photographs shown in Fig. 5, it can be observed that some of the dripping drops are not truly spherical. After detaching from the wire, they appear to be like prolate spheroids with a major axis L_1 and a minor axis L_2. An equivalent drop diameter of a prolate spheroid can be found by equating its volume in the following equation:

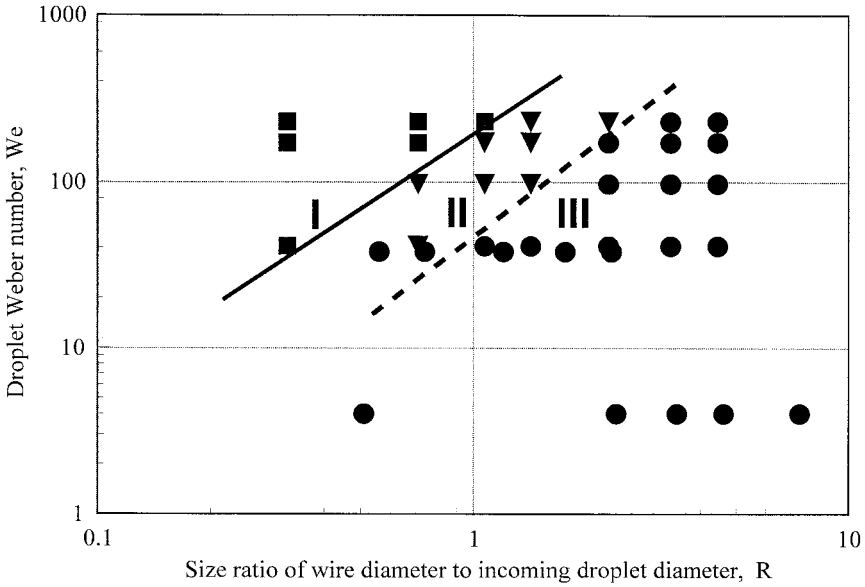

Fig. 7. Regime map of the impacting phenomena.

$$\frac{4}{3}\pi\left(\frac{L_1}{2}\right)\left(\frac{L_2}{2}\right)^2 = \frac{1}{6}\pi(D')^3 \tag{5}$$

Therefore, the equivalent diameter of the dripping drop can be found by the following equation:

$$D' = \sqrt[3]{L_1 L_2^2} \tag{6}$$

This formulation is used for deducing the data from non-spherical dripping drops.

Fig. 8 shows the relationship between the diameter of the dripping drops and the wire size at three Weber numbers of 41, 97 and 230. The typical size range of the dripping drops is between 2.6 and 4.4 mm. In general, a larger dripping drop is associated with a larger wire at a given Weber number condition. The rate of increase gets smaller as the wire size increases. However, as the Weber number increases, the droplets give more downward momentum in addition to the weight of hanging drop to balance with the surface tension. This gives a smaller size of the dripping drops.

The wetting of the surface would affect the interfacial contact and the contact angle between the solid surface and the droplet that would subsequently influence the size of the dripping drops. Therefore, a preliminary study of the droplets impacting on waxed wires has also been performed. As shown in Fig. 8, at the Weber number of 98 and for the wire diameters of 381, 508 and 1190 μm, the dripping drops detached from the waxed wires are about 40% smaller than the ones from the non-waxed wires. This is because when the wire's surface is waxed, the interfacial contact angle between the wire and the liquid film is increased and the net effect of the surface tension is reduced. The film has much less tendency to stick or wet the waxed

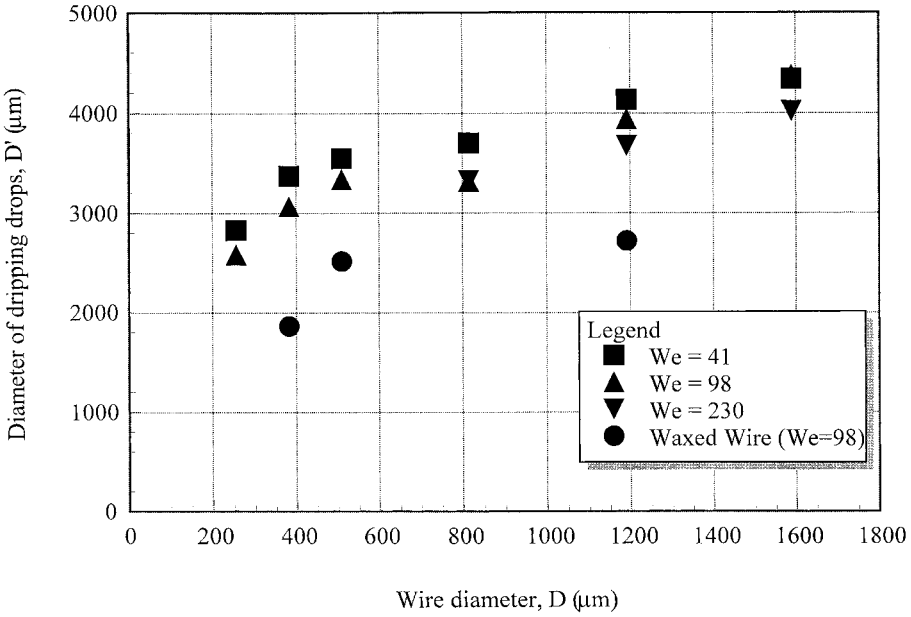

Fig. 8. Plot of size of dripping drop versus wire diameter.

surfaces. Similar observations have also been found on another impaction study in which the droplets impacted onto the non-wetting Teflon wire.

It appears from above that the size of the dripping drop depends on the wire diameter and the geometry of the liquid–solid interfacial contact on the wires. However, due to the complex three-dimensional nature of the pendent drop attaching under the wire, it is impractical to determine a detailed measure of the liquid–solid contact at the interface. Therefore, a simple two-dimensional force balance has been established to predict the size of the dripping drop when it is about to detach from the wire (Fig. 3). If it is assumed that the dripping drop attaches onto the wire over a length of D on both sizes, then the balance between the attachment force and the weight of the drop can be given as:

$$\sigma 2D = \frac{\pi D'^3}{6}\rho \boldsymbol{g} \tag{7}$$

Using the definitions of R' and B as given in (3) and (4), the above equation can be re-written as follows:

$$R' = 1.563B^{-0.667} \tag{8}$$

A relationship can be obtained from (8) between the dripping drop size and the non-dimensional wire Bond number, which is an important parameter because it relates the force balance of surface tension and the gravitational (weight) effect at the bottom surface of the wire. Fig. 9 displays a log–log plot of the size ratio of the dripping drop to the wire diameter (R') versus the wire Bond number (B). All symbols generally fall into linear trends on the log–log plot. It appears that this dripping phenomenon is relatively independent of the Weber

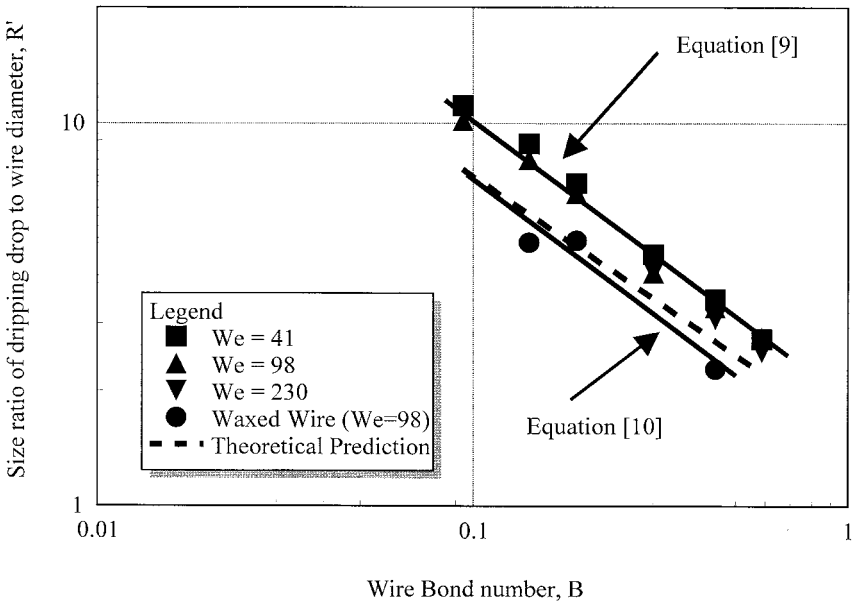

Fig. 9. Plot of R' versus wire Bond number (B).

number condition. The available data was fitted using a least square method and the correlation for the non-waxed wire is found to be:

$$R' = 1.813B^{-0.786} \tag{9}$$

And for the waxed wire impaction at the Weber number of 98, the correlation is:

$$R' = 1.299B^{-0.722} \tag{10}$$

The theoretical dripping size prediction from equation (8) is also plotted on the same figure for comparison. Even though there is a slight difference in the magnitude due to the two-dimensional assumption, the trend of equation (8) correctly resembles those given by the correlations in (9,10). These correlations may be used to predict the dripping size of other similar impacting processes within reasonable limits.

4. Conclusions

Experimental studies of water droplets impacting on cylindrical wires were conducted systematically. The effect of droplet velocity and the wire sizes were varied parametrically to reveal the impaction characteristics. Some concluding remarks of the investigation are listed below:

1. The typical modes of impaction outcome were disintegration and dripping. Smaller droplets were disintegrated if the incoming droplets had higher velocity or the wire diameter was

small. Larger dripping drops were formed when the velocity was low or the wire diameter was large.
2. A non-dimensional map based on the droplet Weber number was developed to identify the different regimes of the disintegration mode, the momentum induced dripping mode, and the gravity induced dripping mode.
3. The sizes of the dripping drops were measured through image processing and were correlated well with reasonable dependency on the wire Bond number. The correlations showed a relatively linear trend on a log–log plot, demonstrating that the Bond number was an important parameter for size measurement of drops dripping under wires.
4. The surface effect was also examined briefly by studying the droplets impacting on waxed wires. The drops dripping from waxed wires were generally smaller than the ones from the non-waxed wires due to the reduced surface tension effect at the interfacial contact.

Acknowledgements

The authors greatly appreciate the funding for this research supported by the US Department of Commerce, National Institute of Standards and Technology, Building and Fire Research Laboratory, under Grant No. 60NANB5D0093.

References

Ashgrizzadeh, N., Yao, S.C., 1983. Development of multiorifice impulsed spray generator for heterogeneous combustion experiments. In: ASME/JSME Thermal Engineering Joint Conference Proceedings, 2, pp. 429–433.

Bussmann, M., Chandra, S., Mostaghimi, J., 1997. Droplet impact onto arbitrary surface geometries. In: Proceedings of ASME Fluids Engineering, FEDSM97, 3073.

Cazabat, A., 1987. How does a droplet spread? Contemp. Phys. 28, 347–364.

Chandra, S., Avedisian, C.T., 1991. On the collision of a droplet with a solid surface. Proc. R. Soc. Lond. A 432, 13–41.

Cohen, R.D., 1991. Shattering of a liquid drop due to impact. Proc. R. Soc. Lond. A 435, 483–503.

Crease, G.J., Hall, F.R., Thacker, J.R.M., 1991. Reflection of agricultural sprays from leaf surfaces. J. Environ. Sci. Health B26 (4), 383–407.

Dear, J.P., Field, J.E., 1988. High-speed photography of surface geometry effects in liquid/solid impact. J. Appl. Phys. 63, 1015–1021.

Fukai, J., Shiiba, Y., Yamamoto, T., Miyatake, O., Poulikakos, D., Megaridis, C.M., Zhao, Z., 1995. Wetting effects on the spreading of a liquid droplet colliding with a flat surface: experiment and modeling. Phys. Fluids 7 (2), 236–247.

Harlow, F.H., Shannon, J.P., 1967. The splash of a liquid drop. J. Appl. Phys. 38 (10), 3855–3866.

Hislop, E.C., 1988. Electrostatic ground-rig spraying: an overview. Weed Technol. 2, 94–105.

Hung, L.S., 1998. Investigation of the Transport and Dynamics of Droplets Impacting on Complex Objects, Carnegie Mellon University, Pittsburgh, PA (Ph.D. Thesis).

Karl, A., Anders, K., Frohn, A., 1994. Experimental investigation of droplet deformation during wall collisions by image analysis. In: Proceedings of ASME Winter Annual Meeting, FED-Vol. 172, pp. 135–141.

Lesser, M.B., 1981. Analytic Solutions of liquid-drop impact problems. Proc. R. Soc. Lond. A 377, 289–308.

Levin, A., Hobbs, P.V., 1971. Splashing of water drops on solid and wetted surfaces: Hydrodynamics and charge separation. Phil. Trans, R. Soc. London A 269, 555–585.

Liu, H., Lavernia, E.J., Rangel, R.H., 1994. Modeling of molten droplet impingement on a non-flat surface. In: Proceedings of ASME Fluid Engineering, FED-Vol. 201, pp. 1–5.

Rein, M., 1993. Phenomena of liquid drop impact on solid and liquid surfaces. Fluid Dyn. Res. 12, 61–93.

Reichard, D.L., Brazee, R.D., Bukovac, M.J., Fox, R.D., 1986. A system for photographically studying droplet impaction on leaf surface. Trans. ASAE 29 (3), 707–713.

Spillman, J.J., 1984. Spray impaction, retention and adhesion: an introduction to basic characteristics. Pestic. Sci. 15, 97–106.

Yao, S.C., Cai, K.Y., 1988. The dynamics and Leidenfrost temperature of drops impacting on a hot surface at small angles. Exp. Therm. Fluid Sci. 1, 363–371.

Yao, S.C., Hochreiter, L.E., Cai, K.Y., 1988. Dynamics of droplets impacting on thin heated strips. J. Heat Transfer 110, 214–220.

Zhao, Z., Poulikakos, D., Fukai, J., 1996a. Heat transfer and fluid dynamics during the collision of a liquid droplet on a substrate—I. Modeling. Int. J. Heat Mass Transfer 39, 2771–2789.

Zhao, Z., Poulikakos, D., Fukai, J., 1996b. Heat transfer and fluid dynamics during the collision of a liquid droplet on a substrate—II. Experiments. Int. J. Heat Mass Transfer 39, 2791–2802.